FTIR Investigation of the Fluorocyclohexane Ring Inversion in Liquid Kr

Alexandr I. Fishman,† Wouter A. Herrebout, and Benjamin J. van der Veken*

Universitair Centrum Antwerpen, Groenenborgerlaan 171, B-2020 Antwerpen, Belgium

Received: December 10, 2001; In Final Form: February 12, 2002

Midinfrared spectra of solutions of fluorocyclohexane, $C_6H_{11}F$, in liquid Kr (LKr) have been investigated at temperatures between 120 and 188 K. Three temperature intervals are distinguished for the equatorial (e) ⇌ axial (a) conformational relaxation. At temperatures below 141 K the rate of conformational equilibration is negligible and the population ratio of the conformers is "frozen", while at temperatures above 151 K the equilibrium is established nearly instantaneously. In the intermediate temperature interval, the relaxation times are such that the equilibration can be followed using FTIR spectroscopy. From spectra recorded between 151 and 188 K the standard enthalpy difference $\Delta H°$ in LKr was determined to be 1.3 (4) kJ mol^{-1}. Between 141 and 151 K, and starting from solutions with nonequilibrium conformer populations, the conformational relaxation was studied as a function of time. From these data, the enthalpy $\Delta H^{‡}$ and entropy $\Delta S^{‡}$ of activation for the a- to e-conformer interconversion were found to be 37.8 (12) kJ mol^{-1} and −30 (9) J mol^{-1} K^{-1}, respectively. From the kinetic data, the extinction coefficients ratio ϵ_e/ϵ_a for the ν_{21} conformational doublet was determined to be 0.38 (4). The standard entropy difference $\Delta S°$ was determined using this extinction coefficient ratio, yielding a value of 1.14 (11) J mol^{-1} K^{-1}, and was also determined from the temperature dependence of the infrared band areas, yielding a value of 1.0 (6) J mol^{-1} K^{-1}. The results are discussed in light of literature data and in light of Monte Carlo free energy perturbation calculations, which yield information on the difference in solvation enthalpy and difference in solvation entropy of this species studied.

Introduction

Cyclohexane and monosubstituted cyclohexanes are conformationally flexible systems, and the conformational equilibrium in these molecules has been the subject of intense research.[1−15]

In this study we concentrate on dynamic aspects of fluorocyclohexane (FCH). This compound has been studied by different physical methods. It was shown that, in the gas phase, in the pure liquid, and in solutions, FCH occurs as a mixture of two different chair conformers, with the fluorine atom either in an equatorial (e) or in an axial (a) position. Electron diffraction[1] and microwave[2,3] studies yielded gas-phase values of the standard Gibbs energy difference $\Delta G°$ of 0.71 (at 298 K)[1] and 1.25 (12) kJ mol^{-1} (at 187 K).[3] FCH has been investigated repeatedly by NMR spectroscopy.[4−11] No significant phase dependence of the e−a conformational equilibrium constant was observed: the gas-phase value of $\Delta G°$ at 250 K[8] is 1.05 (6) kJ mol^{-1} and the liquid-phase value is 0.88 kJ mol^{-1} at 250 K[10] and 0.75 kJ mol^{-1} at 298 K.[4] It was further shown[4] that in solution $\Delta G°$ is remarkably independent of the solvent, the different values ranging from 0.38 kJ mol^{-1} in nitrobenzene to 0.84 kJ mol^{-1} in acetic acid (at 298 K).

The vibrational spectra of FCH have also been investigated.[12−15] A detailed analysis of the infrared and Raman spectra was carried out by Christian et al.[15] In this study, the midinfrared and far-infrared spectra of the vapor, liquid, and solid phases were recorded, while high-pressure data on the neat liquid and on CS_2 solutions were obtained using a diamond anvil cell. Also, Raman spectra of the liquid and of the amorphous and crystalline solids at various temperatures were presented. In agreement with the conclusions derived from other spectroscopic studies, the data obtained by Christian et al.[15] show the presence of a- and e-conformers in the vapor and liquid phases, and in the plastic solid state.

Vibrational spectroscopy can be used to determine the activation parameters for conformational interconversion. Procedures to derive liquid-phase values for these parameters have been described.[16−18] In these studies, the kinetics of conformational transitions were studied by dissolving the molecules in liquefied gases such as ethane, propane, and some Freons. More recently, this technique has been expanded by using solutions in liquid rare gases.[19] The latter solvents have the advantage of having greater chemical inertness, and of being transparent in a much wider spectral region, from the far-infrared up to the UV. Satisfactory liquid phase temperature intervals can easily be achieved at slightly increased pressures.[20,21]

In the present paper we describe the results of a kinetic study of the fluorocyclohexane ring inversion in liquid Kr (LKr) using infrared spectroscopy. From the data, the enthalpy $\Delta H^{‡}$ and entropy $\Delta S^{‡}$ of activation were determined. In addition, the standard enthalpy difference $\Delta H°$ and the standard entropy difference $\Delta S°$ describing the conformational equilibrium were measured in the same solvent.

Experimental Section

The sample of FCH was obtained from Lancaster Synthesis (purity 98+%) and was used without further purification. The krypton was obtained from L'Air Liquide and had a stated purity of 99.998%.

The infrared spectra were recorded using a Bruker IFS 66v spectrometer equipped with a globar source, a Ge/KBr beam

* Corresponding author. Fax: +32 3 2180233. E-mail: bvdveken@ruca.ua.ac.be.

† On leave from Kazan State University, Kazan, Kremlevskaya str.18, 420008, Russia.

10.1021/jp0144855 CCC: $22.00
Published on Web 04/17/2002

splitter, and a liquid nitrogen cooled broad band MCT detector. The interferograms were recorded with a resolution of 0.5 cm^{-1} and Fourier transformed using a Blackman-Harris apodization function. A zero-filling factor of 4 was used for all experiments. The number of scans used in a particular experiment was varied from 50 to 250, depending on the rate of interconversion that was followed spectroscopically.

The cell for liquids used in this study is made of stainless steel, has a path length of 70 mm, and is equipped with wedged silicon windows. The cell is designed for use at pressures up to 150 bar[21] and is cooled with bursts of liquid nitrogen. The temperature of the cell is measured by a Pt-100 thermoresistor.

The study of conformational interchanges and the corresponding reaction rates requires the production of a solution in which the conformer population is sufficiently displaced from equilibrium. In this study, such solutions were prepared in the following way. A steel vessel with an approximate volume of 200 cm^3 was filled at room temperature with a gaseous mixture of FCH and Kr, with a mole fraction ratio close to 1:3500. This mixture was rapidly condensed into the cell, which had been cooled to 120 K. This results in a solution of FCH in LKr in which the relative conformer populations are close to their room-temperature equilibrium values. Subsequently, an additional amount of krypton was added to ensure complete filling of the cell. The resulting mole fraction of FCH is estimated to be 1:4500. After homogenizing at 130 K during 1 h, the cell was heated to the temperature required, and IR spectra were recorded under isothermal conditions. During all experiments, the temperature of the cell was controlled manually, which resulted in a standard deviation of the temperature smaller than 0.3 K.

For the quantitative analysis band areas of spectral bands belonging to the a-conformer and the e-conformer were obtained from least-squares fittings using Gauss/Lorentz sum functions. These calculations were performed using Peakfit 4.01.[22] Linear and nonlinear regression analysis of the data derived from the vibrational spectra were carried out using Origin 6.0.[23] All uncertainties reported are standard deviations.

Differences in solvation Gibbs energies were obtained from Monte Carlo free energy perturbation calculations, in which the interconversion of one conformer into another in liquid krypton is simulated, using BOSS 4.1.[24] All simulations were run in the NPT ensemble, using a cubic box and periodic boundary conditions. A box containing 1 solute molecule and 256 Kr atoms was used, while preferential sampling was introduced to describe the displacements of the solute atoms. During all calculations, attempts to move the solute molecule were made on every 50th configuration, while volume changes were applied on every 500th configuration. The ranges for the attempted changes were chosen to provide a 40% accepted probability.

The path from $\lambda = 0$ (axial conformer) to $\lambda = 1$ (equatorial conformer) was completed in 40 steps, each step corresponding to a change $\Delta\lambda$ equal to 0.025. Advantage was taken of double-wide sampling allowing the calculations of two Gibbs energy changes at each step, i.e., between a reference system at which the simulations are performed ($\lambda = \lambda_0$) and two perturbed systems with $\lambda = \lambda_0 \pm \Delta\lambda$. Each calculation consisted of an equilibrium phase of 10.0×10^6 configurations and a production phase of 40.0×10^6 configurations.

Results

The vibrational frequencies of FCH dissolved in LKr agree favorably with those reported for the liquid and vapor phases,[15] which made assignments straightforward. The frequencies, characterizing the a- and e-conformers, that are used below, and their assignments, are summarized in Table 1.

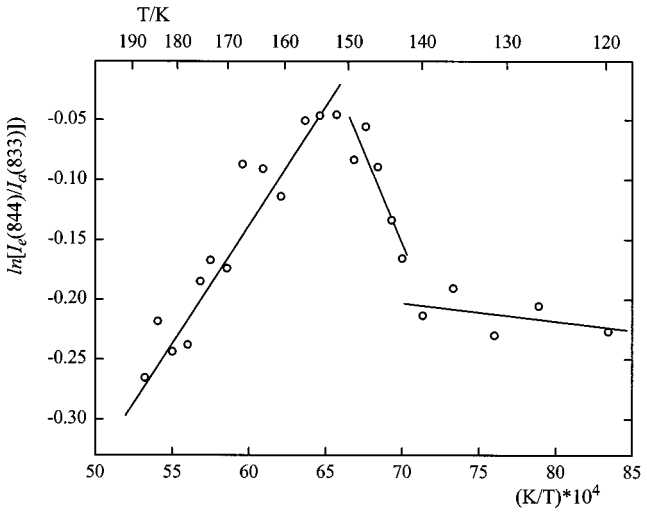

Figure 1. Plot of the logarithm of the ratio of the infrared band areas of the 844 (e-conformer) and 833 cm^{-1} (a-conformer) bands vs $1/T$ for fluorocyclohexane dissolved in LKr. Temperature of the sample increased gradually from 120 to 188 K.

TABLE 1: Characteristic Vibrational Frequencies for the a- and e-Conformers of Fluorocyclohexane

IR band maximum/cm^{-1}			
solution in LKr	liquid[15]	conformer	assignt[15]
833.3	830	a	ν_{21}
844.7	844	e	ν_{21}
866.7	865	a	ν_{20}, ν_{44}
1191.0	1190	e	ν_{39}
1330.5	1328	e	ν_{13}
		a	ν_{37}
1341.0	1339	a	ν_{12}, ν_{13}, ν_{36}

Kinetic Results. The activation Gibbs energy of conformational transitions can be determined from measurements, at different temperatures, of the rate constants of the conformer equilibration reactions. It has been shown[16−19,25,26] that three temperature ranges can be distinguished for a conformational relaxation process. In the lowest temperature range the rate constants for conformational interchange are very small and the population ratio of the conformers for all intents and purposes may be taken to be "frozen". In the highest temperature interval, the equilibrium is established "instantaneously". In the intermediate temperature range, the relaxation times are such that the equilibration can be followed with standard FTIR techniques.

This is illustrated in Figure 1, in which the logarithm of the ratio $I_e(844)/I_a(833)$ of the band areas of the 844 and 833 cm^{-1} infrared bands of a solution of FCH in LKr is shown as a function of the inverse temperature. The data were obtained by recording spectra of a solution that was heated at a constant rate of approximately 15 K/h. The three different temperature intervals can be clearly distinguished. At temperatures below 141 K, $\ln[I_e(844)/I_a(833)]$ hardly varies. Obviously in this range the rate of conformational equilibration is negligible: the nonzero slope of the regression line is due to the temperature variation of the extinction coefficient ratio. In contrast, at temperatures above 151 K, $\ln[I_e(844)/I_a(833)]$ shows a linear dependence upon the inverse temperature, showing that the equilibrium is established on a time scale small compared with the time scale of the experiment, thus yielding conformer populations which are in agreement with the van't Hoff isochore.[27] In the temperature range between 141 and 151 K,

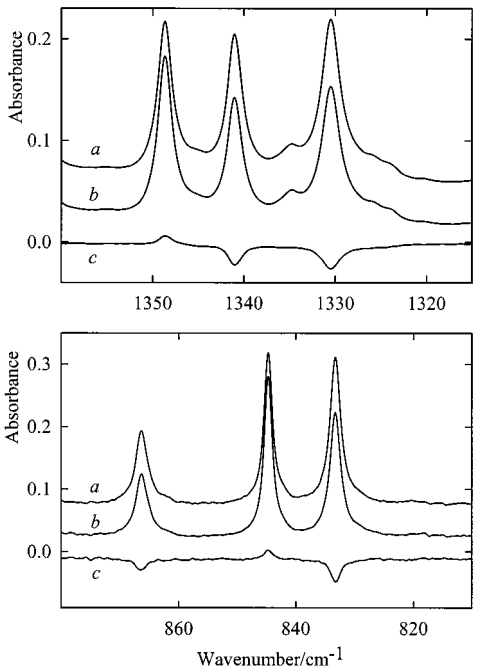

Figure 2. Infrared spectra of fluorocyclohehane dissolved in LKr at 136.6 K. (a) Nonequlibrium and (b) equilibrium mixture of the conformers. (c) Difference between b and a.

irreversible changes are observed, which indicate that in this interval the relaxation process can be followed spectroscopically. This temperature interval was used for kinetic investigations.

In Figure 2, the 1360−1315 and the 880−815 cm^{-1} regions obtained for a typical solution of FCH in LKr at 136.6 K are shown. For both plots, trace a is the spectrum of the solution obtained immediately after the selected temperature was obtained, while trace b is the spectrum of the same solution recorded 3 h later. Trace c is the difference spectrum obtained by subtracting (b) from (a). It can be seen that during the relaxation the band areas of the 1341 and 833.3 cm^{-1} a-modes decrease, while that of the 844 cm^{-1} e-mode increases. A decrease of magnitude similar to that of the 1341 cm^{-1} band is observed for the band at 1330.5 cm^{-1}. This band has been assigned to both ν_{13} of the e-conformer and ν_{37} of the a-conformer, so that the observed decrease implies that the contribution of ν_{13}(e) is considerably smaller that that of ν_{37}-(a). It should also be noted that the increase of the band area for the 844 cm^{-1} (ν_{21}(e)) band is significantly smaller than the decrease observed for the 833 cm^{-1} (ν_{21}(a)) band. Because the changes in concentration observed for the a-conformer and the e-conformer are equal in magnitude, but different in sign, the unequal changes must reflect significant differences in the extinction coefficients of the bands. This will be discussed in more detail in a later paragraph.

Measurement of k_a and k_e. The interconversion

$$e \rightleftharpoons a \tag{1}$$

between the e- and a-conformers can be described as a first-order monomolecular reversible reaction.[18] The kinetic equations describing the changes of the concentrations c_a and c_e of the conformers in such a reaction are given by

$$dc_a/dt = -dc_e/dt = -k_a c_a + k_e c_e \tag{2}$$

where k_a and k_e are the rate constants for the a → e and e → a interconversions, respectively. If the total concentration, $c = c_a + c_e$, remains constant during the experiment, the solution

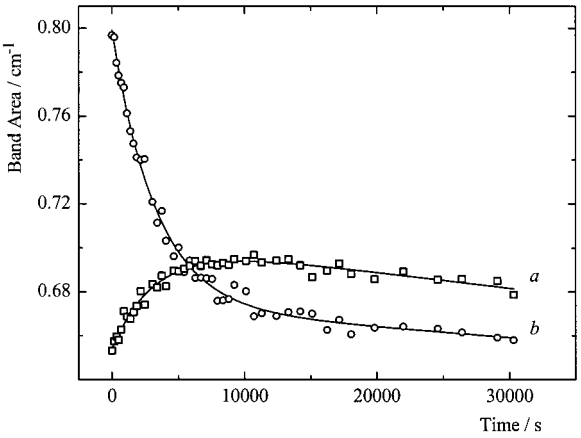

Figure 3. Band areas of 844.7 (a) and 833.3 cm^{-1} (b) bands of fluorocyclohexane in LKr at 136.6 K as a function of time. The solid lines give the behavior as simulated by eq 4.

for an isothermal process described by eq 2 is given by

$$c_a(t) = c_a^{\infty} - (c_a^{\infty} - c_a^{0}) \exp[-(k_a + k_e)t] \tag{3}$$

where c_a^0 is the concentration of the a-conformer in the beginning of the relaxation process ($t = 0$) and c_a^{∞} is the equilibrium concentration ($t \rightarrow \infty$), with a completely analogous expression for the e-conformer.

Expression 3 shows that at the end of the relaxation process the concentrations of the conformers should become constant. The resulting values for c_a^{∞} and c_e^{∞} define the equilibrium constant K at the temperature studied:

$$K = k_e/k_a = c_a^{\infty}/c_e^{\infty} = (\epsilon_e/\epsilon_a)/(I_e^{\infty}/I_a^{\infty}) \tag{4}$$

where ϵ_e and ϵ_a are the extinction coefficients of the e- and a-conformers, respectively, and I_e^{∞} and I_a^{∞} are the equilibrium concentrations.

By combining the results obtained for c_e^{∞} and c_a^{∞}, eq 4, and the results obtained for $k_a + k_e$, eq 3, and via a measurement of ϵ_e/ϵ_a, the values of k_a and k_e can be determined separately.

In Figure 3, the band areas of the 844 and 833 cm^{-1} bands obtained during an isothermal study at 136.6 K are shown as a function of time. It can be seen that, in the initial phase of the experiment, the band area of the 833 cm^{-1} band decreases, while that of the 844 cm^{-1} band increases. The data also show that, from $t = 10\,000$ s onward, the band areas of both bands decrease, by some 1.5%. This suggests that, in addition to the relaxation process, a second process is taking place, which leads to a decrease of both concentrations c_e and c_a. The reasons for this decrease are not fully understood, but possible contributions are a decomposition of FCH and/or a partial crystallization of FCH on the cell walls. These hypotheses, however, are not supported by the detection in the spectra of bands due to decomposition products or due to crystallites.

Because the band areas of both the 844 and 833 cm^{-1} bands do not converge to a constant value, the model described by eq 3 cannot be used for the analysis of the present experimental data. Therefore, a new model was developed, in which the small changes of the concentration are taken into account explicitly. The data in Figure 3 illustrate that at the end of the relaxation process the time evolution of the band areas is very nearly linear. This implies a similar nearly linear behavior of the total concentration c, which can be approximated as

$$c = c_a + c_b = A + Bt \tag{5}$$

TABLE 2: Resulting Values of the Sum of the Rate Constants $k_a + k_e$ Fitted Using Eq 4

temp/K	frequency/cm^{-1}	$(k_a + k_e) \times 10^3$/s^{-1}
136.6	1341.0 a[a]	0.30 (1)
	1330.5 e, a	0.32 (1)
	844.7 e	0.31 (3)
	833.3 a	0.31 (2)
138.2	1341.0 a	0.52 (4)
	1330.5 e, a	0.45 (5)
	1191.0 e	0.39 (4)
	844.7 e	0.47 (5)
	833.3 a	0.46 (3)
140.7	1341.0 a	0.97 (5)
	1330.5 e, a	0.99 (6)
	1191.0 e	0.75 (10)
	844.7 e	0.84 (11)
	833.3 a	1.04 (7)
143.2	1341.0 a	1.8 (2)
	866.7 a	1.6 (4)
	844.7 e	1.3 (2)
	833.3 a	2.0 (2)
147.8	1341.0 a	3.9 (5)
	1330.5 e, a	4.2 (4)
	844.7 e	3.4 (17)
	833.3 a	5.3 (8)

[a] The letters "e" and "a" refer to the conformer to which the band used is assigned.

where A and B are constants, and the differential equation describing the changes in c_a can be modified as

$$dc_a/dt + (k_a + k_e)c_a = k_e(A + Bt) \quad (6)$$

For an isothermal process such as that observed in this study, eq 6 has a solution:

$$c_a(t) = p_1 \exp[-(k_a + k_e)t] + p_2 + p_3 t \quad (7)$$

in which p_1, p_2, and p_3 are constants. It may be safely assumed that, with the concentrations used, the extinction coefficients of infrared bands are not affected during isothermal time runs, so eq 7 can be used to model the behavior of band areas such as those shown in Figure 3. Therefore, we have used an equation of the form (7) to analyze, using nonlinear least-squares fitting,[23] the temporal evolution of the band areas of several bands of FCH, at five different temperatures between 136.6 and 147.8 K. The sum rate constants $k_a + k_e$ obtained have been collected in Table 2. It can be seen that at every temperature the values are equal within their uncertainty limits. The quality of the fits is illustrated for the 844 and 833 cm^{-1} bands at 136.6 K in Figure 3, in which the optimized behaviors of the model are shown as solid lines. It may be remarked that the results in Table 2 for the 1330.5 cm^{-1} band are in agreement with those for the other bands. This is not surprising, because the fact that this band is composed of contributions from both conformers does not affect the value of the sum of the rate constants derived from it using eq 7.

Measurement of $\Delta H°$ and ϵ_e/ϵ_a. Using $\Delta G° = G°(a) - G°(e) = \Delta H° - T\Delta S°$, the standard entropy difference between the conformers, $\Delta S°$, can be calculated if $\Delta G°$ and $\Delta H°$ are known. The standard enthalpy difference $\Delta H°$ was derived using the van't Hoff isochore.[27] The other contribution, $\Delta G°$, can be derived as $\Delta G° = -RT \ln K$, in which K is as defined by eq 4. K can be derived from the experimental ratio I_e^∞/I_a^∞, if the extinction coefficients ratio ϵ_e/ϵ_a is known.

Values for $\Delta H°$ were obtained from several temperature studies in the 150−190 K interval, in which the conformational equilibration is near instantaneous. For each temperature run a van't Hoff plot was constructed using the 844 and 833 cm^{-1} band areas. The standard enthalpy differences were calculated from the slopes of the linear regression lines. The values obtained from five different temperature studies varied between 0.97 and 1.90 kJ mol^{-1}, with an average $\Delta H°$ of 1.3(4) kJ mol^{-1}. This value is close to the value of 0.9(3) kJ mol^{-1} reported[11] for a solution of FCH in CS_2. It confirms the conclusion[4] that the conformational equilibrium in FCH is remarkably independent of the solvent.

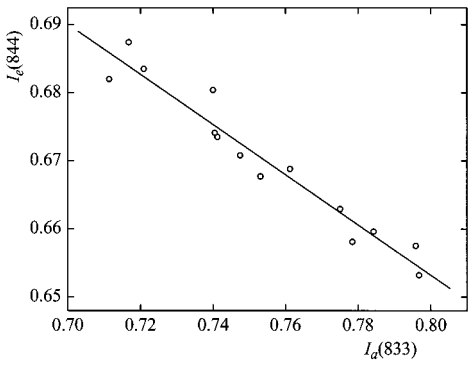

Figure 4. Dependence of the band area $I_e(844)$ of the 844 cm^{-1} band on that of the 833 cm^{-1} band, $I_a(833)$, at 136.6 K.

If the total concentration remains constant during the isothermal process, the value of the extinction ratio ϵ_e/ϵ_a can be obtained from a plot of the band area of the equatorial band, I_e, versus that of the axial band I_e:[16,18]

$$I_e = -(\epsilon_e/\epsilon_a)I_a + \epsilon_e lc \quad (8)$$

where l is the thickness of the absorbing layer. It follows from the above that the requirement of a constant total concentration is not strictly fulfilled for the present measurements. However, the errors introduced by neglecting the changes in concentration are relatively small, as can be seen from the following. During the experiment, the relative change of the total concentration of the solution can be written as

$$\frac{dc}{c} = \frac{(dI_e/\epsilon_e) + (dI_a/\epsilon_a)}{(I_e/\epsilon_e) + (I_a/\epsilon_a)} \quad (9)$$

Inspection of the data in Figure 3 shows that during the last 5 h of the isothermal study the changes in I_e and I_a are nearly identical, i.e., $dI_e(844) \approx dI_a(833)$, while the intensities for I_e and I_a are quite similar, i.e., $I_e(844) \approx I_a(833)$. From eq 9 then follows

$$\frac{dc}{c} \approx \frac{dI_e}{I_e} < 0.015 \quad (10)$$

If it is assumed that the rate of change of the concentration during the first hour is similar to that in the final 5 h, it follows that during the first hour the change in the total concentration is limited to 0.3%. Such a small change can be neglected, from which follows that a reasonable estimate of the ratio ϵ_e/ϵ_a can be obtained using data from that time interval.

In Figure 4, the 844 and 833 cm^{-1} band areas obtained during the first hour of the isothermal study at 136.6 K are plotted against each other. In line with the above assumption, the data are linearly related. Similar analyses were also carried out for the other isothermal experiments. The values for ϵ_e/ϵ_a obtained from these studies vary between 0.33(4) and 0.44(3) and yield an average value of 0.38(4).

The above value of ϵ_e/ϵ_a for the 844/833 cm^{-1} conformational doublet is corroborated by ab initio calculations. The frequencies for ν_{21} (Table 1) obtained from density functional calculations at the B3LYP/6-311++G(d,p) level are 855 cm^{-1} for the e-conformer and 847.5 cm^{-1} for the a-conformer, while the corresponding infrared intensities are 1.0 and 3.9 km mol^{-1}, respectively. Thus, the calculations confirm that the extinction coefficient for the e-conformer is significantly smaller than that for the a-conformer, even if the calculated ratio, 0.26, is somewhat smaller than the experimental value 0.38(4).

Measurement of $\Delta S°$. Values for $\Delta S°$ were derived by two different methods. In the first, $\Delta S°$ was calculated from $\Delta G°$ and $\Delta H°$, as described in the previous paragraph. Using eq 4 and the average value of ϵ_e/ϵ_a derived above, values of $\Delta G°$ and $\Delta S°$ were calculated for the time runs given in Table 2. The individual values of $\Delta G°$ ranged from 1.12 to 1.15, with an average of 1.14(2) kJ mol^{-1}, while the values of $\Delta S°$ ranged from 1.01 to 1.28, with an average of 1.14(11) J mol^{-1} K^{-1}.

In the second method, $\Delta S°$ is derived by combining data from the highest and lowest temperature ranges of the experiments such as the one shown in Figure 1. In the first interval both conformers are in equilibrium and the ratio of the band areas are determined by the van't Hoff isochore. In the second interval no conformational changes occur, so the band areas hardly vary with temperature.[17,18,28] The band areas in this temperature interval can, therefore, be written as

$$I_e^c = \epsilon_e l c_e^c,\ I_a^c = \epsilon_a l c_a^c \tag{11}$$

where constant concentrations c_e^c and c_a^c refer to some temperature T_0, called the "temperature of freezing",[18] at which the ratio c_e^c/c_a^c is the equilibrium ratio of the conformer populations. From the relationships

$$\frac{c_a}{c_e} = \exp(\Delta S°/R)\exp(-\Delta H°/RT),$$

$$\frac{c_a^c}{c_e^c} = \exp(\Delta S°/R)\exp(-\Delta H°/RT_0) \tag{12}$$

and $c_a + c_e = c_a^c + c_e^c$, the following expression can be derived:

$$Y = \exp(\Delta S°/R)X \tag{13}$$

where the variables X and Y are defined as

$$X = \frac{I_e^c}{I_e}\exp(-\Delta H°/RT_0) - \exp(-\Delta H°/RT) \text{ and } Y = 1 - \frac{I_e^c}{I_e} \tag{14}$$

Relation 13 reveals a linear dependence of Y on X, and $\Delta S°$ can be calculated from the slope.

For the present study five experiments were performed, each starting from a fresh vapor-phase mixture. The solutions were prepared at 185 K. After homogenizing at that temperature for 30 min, a spectrum was recorded. Subsequently, the temperature of the solution was decreased stepwise, by approximately 3−4 K in each step. After each step the temperature was equilibrated and a new spectrum was recorded. This was repeated until the final temperature, 118 K, was reached.

Band areas for the equatorial 844 cm^{-1} band obtained in the high- and low-temperature interval of a typical temperature run

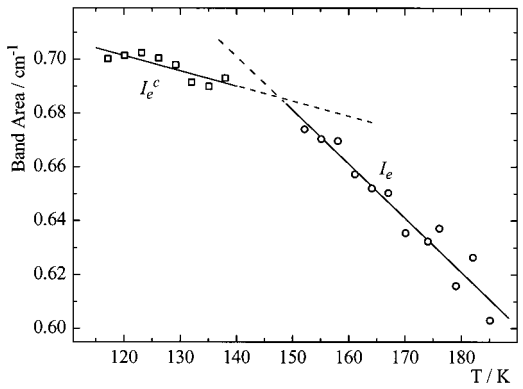

Figure 5. Temperature dependencies of the band area $I_e(844)$ and $I_e^c(844)$ of fluorocyclohexane dissolved in LKr. $I_e = 0.98_{0.03} - (20.1_{1.6})10^{-4}T$ (solid line); $I_e^c = 0.769_{0.019} - (5.7_{1.4})10^{-4}T$ (solid line), $T_0 = 148$ K.

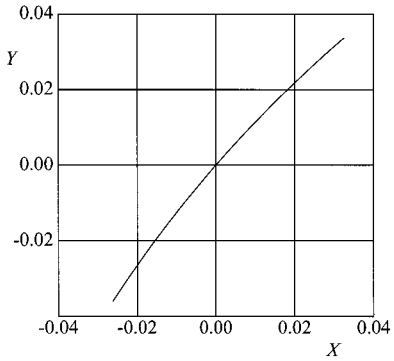

Figure 6. Dependence of Y as a function of X, where $Y = 1 - (I_e^c/I_e)$ and $X = (I_e^c/I_e)\exp(-\Delta H°/RT_0) - \exp(-\Delta H°/RT)$. The parameters I_e and I_e^c are shown in the caption to Figure 5.

are shown in Figure 5. It can be seen that in both intervals a linear relation between band area and temperature may be assumed. The linear regression lines for both intervals are also given. The temperature of their intersect is defined as T_0.

Relations 14 show that X and Y are calculated from the band areas I_e^c and I_e. For temperatures above T_0, where X is negative, I_e is obtained by interpolating the high-temperature regression line and I_e^c is obtained by extrapolating the low-temperature regression line; at temperatures below T_0, where X is positive, interpolation of the low-temperature regression line yields I_e^c and extrapolation of the high-temperature regression line yields I_e.

It may be noted that in the procedure described above there is no need to correct for the changes in solvent densities observed while heating the solution in LKr and/or the changes for the path length due to thermal expansion of the cell, because the definitions of X and Y involve a reduced band area, I_e^c/I_e.

The dependence of Y on X for a typical experiment is shown in Figure 6. The dependence of Y on X can be seen to be nearly linear. The small nonlinearity is due to the fact that at temperatures near T_0 both branches of Figure 5 were approximated by straight lines. The value of $\Delta S°$ for each experiment was calculated from the first derivative dY/dX at $X = 0$.

The values of $\Delta S°$ obtained from this method vary between 1.82 and 0.38 J mol^{-1} K^{-1}, with the average over the five experiments equal to 1.0(6) J mol^{-1} K^{-1} (Table 3). This value is consistent with that obtained from the first method, albeit its uncertainty is significantly bigger. Therefore, in the further analysis below, we will use the more accurate of the two values, 1.14(11) J mol^{-1} K^{-1}, as $\Delta S°$ in LKr.

TABLE 3: Axial−Equatorial Standard Entropy Difference ($\Delta S°$, J mol^{-1} K^{-1}), Standard Enthalpy Difference ($\Delta H°$, kJ mol^{-1}), and Standard Gibbs Energy Difference ($\Delta G°$, kJ mol^{-1}) between the Conformers, and Activation Entropy ($\Delta S_a^{\ddagger}$ and $\Delta S_e^{\ddagger}$, J mol^{-1} K^{-1}) and Activation Enthalpy ($\Delta H_a^{\ddagger}$ and $\Delta H_e^{\ddagger}$, kJ mol^{-1}) for Conformational Transitions of Fluorocyclohexane

environment	$\Delta S°$	$\Delta H°$	$\Delta G°$	$\Delta S_a^{\ddagger}$	$\Delta S_e^{\ddagger}$	$\Delta H_a^{\ddagger}$	$\Delta H_e^{\ddagger}$
liquid krypton	1.14 (11), 1.0 (6)	1.3 (4)	1.14 (2) (140 K)	−30 (9)	−31 (9)	37.8 (12)	39.0 (12)
vapor phase			1.05 (6) (250 K)[8]	13.8 (54)[8]		48.5 (54)[8]	
			1.25 (12) (187 K)[3]				
			0.71 (298 K)[1]				
neat liquid			0.88 (250 K)[10]				
			0.75 (298 K)[4]				
CS_2	−2.9 (17)[11]	0.9 (3)11	1.8 (8) (298 K)[11]				
			1.16 (6) (187 K)[5]				
$CS_2 + (CH_3)_2CO + CD_3OD +$ FCH (1:1:3:5)			1.59 (183 K)[7]				
CCl_3F				−3 (2)[10]		40.1 (4)[10]	
CF_2Cl_2			1.5 (1) (180 K)6				
solid thiourea				−12 (11)[9]		39 (3)[9]	

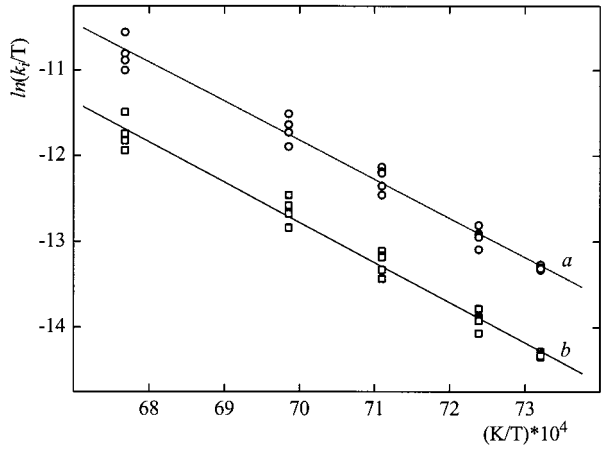

Figure 7. Plots of $\ln(k_a/T)$ (a) and $\ln(k_e/T)$ (b) versus $1/T$ for fluorocyclohexane dissolved in LKr. Symbols at the same temperature correspond to different infrared bands.

Transition State Parameters. Transition state theory[27] derives the following relation between a reaction rate constant k_i and the activation enthalpy $\Delta H_i^{\ddagger}$ and entropy $\Delta S_i^{\ddagger}$ of the reaction:

$$k_i(T) = \frac{k_B T}{h} \exp(\Delta S_i^{\ddagger}/R) \exp(-\Delta H_i^{\ddagger}/RT) \qquad (15)$$

in which k_B and h are the Boltzmann's and Planck's constants, respectively. This equation shows that there is a linear relation between $\ln(k_i/T)$ and inverse temperature, and $\Delta H_i^{\ddagger}$ and $\Delta S_i^{\ddagger}$ can be derived from the slope and the intercept of the regression line.

In Figure 7, the plots are given of $\ln(k_e/T)$ and $\ln(k_a/T)$ versus the inverse temperature. In both cases the relationships are seen to be linear. The values obtained from the regression lines for $\Delta S_a^{\ddagger}$ and $\Delta H_a^{\ddagger}$ are −30(9) J mol^{-1} K^{-1} and 37.8(12) kJ mol^{-1}, while those found for $\Delta S_e^{\ddagger}$ and $\Delta H_e^{\ddagger}$ are −31(9) J mol^{-1} K^{-1} and 39.0(12) kJ mol^{-1}, respectively.

The data in Table 3 show that the activation enthalpy $\Delta H_a^{\ddagger}$ for the solution of FCH in LKr is close to its value in solutions in CCl_3F and in solid thiourea, but it differs substantially from the value in the vapor phase. The observed phase dependence is consistent with an activation volume for the ring inversion process, which is negative.[29]

Discussion

Solvent Effects on $\Delta S°$. The vapor-phase value of $\Delta S°$ is the intrinsic entropic characteristic with which our solution value must be compared. Hitherto, this value has not been determined experimentally. However, it is usually assumed to be very small.[3] This was verified by statistical thermodynamics calculations.[30] The moments of inertia and the complete sets of fundamental vibrational frequencies for each conformer required for these were taken from our density functional calculations at the B3LYP/6-311++G(d,p) level. Using these, at a temperature of 140 K $\Delta S°$ was derived to be a mere −0.1 J mol^{-1} K^{-1}. Therefore, we will assume that this quantity is effectively zero. If this is the case, the entropy difference measured here in solution is entirely due to solvation effects. These must derive to a minor extent from the smaller molar volume of the a-conformer, the hard sphere volume of this conformer being 1.5 cm^3 mol^{-1} less than that of the e- conformer,[31] and to a much greater extent from the difference in polarity, the dipole moments for the e- and a-conformers being 2.11 and 1.81 D, respectively.[32]

The above solvent influence on $\Delta S°$ has been assessed from theory, using Monte Carlo free energy perturbation (MC-FEP)[33,34] calculations. These calculations produce the solvation Gibbs energy $\Delta_{sol}G°(i)$ of the chosen conformer i at a preset temperature. This quantity is defined as the change, at constant pressure, of the intermolecular interaction energy caused by the introduction of the solute into the solvent. The most obvious way of determining the solvent influence on the conformational Gibbs energy difference is, therefore, to subtract the solvation Gibbs energies of the two conformers:

$$\Delta\Delta_{sol}G° = \Delta_{sol}G°(\text{axial}) - \Delta_{sol}G°(\text{equatorial}) \qquad (16)$$

Preliminary calculations, however, showed that this procedure is counterindicated. This is due to the similarity of the $\Delta_{sol}G°$ values for the conformers, which means that $\Delta\Delta_{sol}G°$ has a comparatively small value. To determine this quantity with sufficient precision requires that the $\Delta_{sol}G°$ values are obtained with very high relative precision, which imposes unreasonable demands on the MC calculations. Therefore, $\Delta\Delta_{sol}G°$ was obtained in a different way. From the definition of the $\Delta_{sol}G°$ follows that $\Delta\Delta_{sol}G°$ is the change in intermolecular interaction energy when a solution of the equatorial conformer is converted into a solution of the axial conformer. This conversion interchanges the C−H and C−F bands on one apex carbon atom and causes minor changes in bond lengths and angles in the whole molecule. In the procedure adapted, therefore, the conversion was simulated by the stepwise rotation, governed by the coupling parameter λ, of the C−H and C−F bonds around their bisector, from their position in the equatorial to their position in the axial conformer, accompanied by the required changes in bond lengths and bond angles. This path is physically not realistic, which is thermodynamically unimportant, but it ensures that with every increase of the coupling parameter λ

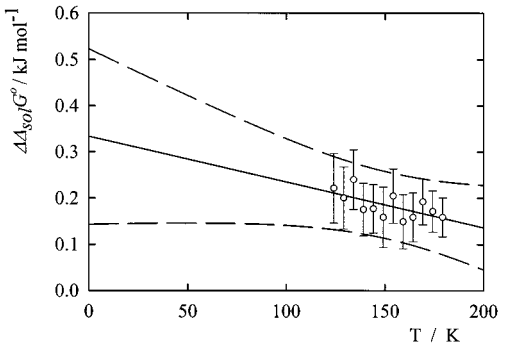

Figure 8. Calculated values for the difference in Gibbs energy of solvation, $\Delta\Delta_{sol}G°$, as a function of temperature. The solid line is the linear regression line, while the dashed lines refer to the corresponding 99% confidence intervals. The error margins given for each data point correspond to 2σ.

the disturbance of the solution is small, so a well converged Gibbs energy change is obtained with an acceptable calculational effort.

Using this procedure, $\Delta\Delta_{sol}G°$ was calculated at 12 different temperatures in the interval between 130 and 180 K. Their values are shown as a function of temperature in Figure 8. The intercept of the linear regression line through the data in this figure equals the solvent influence on $\Delta\Delta_{sol}H°$, the conformational enthalpy difference, and is found to be 0.33(6) kJ mol^{-1}. The negative of the slope of the regression line corresponds to $\Delta\Delta_{sol}S°$, for which a value of 1.0(4) J mol^{-1} K^{-1} is derived. Taking into account the approximations made for the MC-FEP calculations, the agreement between this value and the result obtained above, 1.14(11) J mol^{-1} K^{-1}, is excellent. This may be taken to lend support to the experimental value derived in this study.

Finally, these calculations also allow assessment of the solvent effect on the conformational enthalpy difference. Using the value for the vapor-phase $\Delta H°$, derived by molecular mechanics calculations,[11] 0.80 kJ mol^{-1}, and our value for liquid krypton, 1.3(4) kJ mol^{-1}, the solvent effect $\Delta\Delta_{sol}H°$ is found to be 0.5-(4) kJ mol^{-1}, which compares favorably with the MC-FEP value of 0.33(6) kJ mol^{-1}.

Conclusions

Midinfrared spectra of solutions of fluorocyclohexane in liquid Kr have been investigated at temperatures between 120 and 188 K. In this temperature interval the relaxation rate of the conformer populations changes dramatically: at temperatures below 141 K the rate is negligible and the concentration ratio of the conformers is "frozen", while at temperatures above 151 K the equilibrium is established nearly instantaneously. Analyses of the spectra in the latter temperature interval allowed determination of the standard enthalpy difference. In the 136.6−147.8 K temperature interval, the relaxation was followed using FTIR spectroscopy and the enthalpy and entropy of activation for the a- to e-conformer interconversion were found. From the same measurements the extinction coefficients ratio ϵ_e/ϵ_a for the 844/833 cm^{-1} conformational doublet was determined to be 0.38(4), as well as the standard Gibbs energy difference $\Delta G°$ between the conformers and the standard entropy difference $\Delta S°$. The $\Delta S°$ value was also determined from the temperature dependence of the infrared band areas, and within the error margins the results of the two methods are similar. All thermodynamic and activation parameters are collected in Table 3.

Monte Carlo free energy perturbation calculations yielded information on the difference in solvation enthalpy and difference in solvation entropy between the conformers, which are in good agreement with the experimental values.

Acknowledgment. Financial support by the Flemish Community, through the Special Research Fund (BOF), and the Russian Fund of Fundamental Research (Grant N 99-03-190) are gratefully acknowledged. The authors also thank the Fund for Scientific Research (FWO-Vlaanderen) for help toward the spectroscopic equipment used in this study.

References and Notes

(1) Andersen, P. *Acta Chem. Scand.* **1962**, *16*, 2337.

(2) Pierce, L.; Nelson, R. *J. Am. Chem. Soc.* **1966**, *88*, 216.

(3) Scharpen, L. H. *J. Am. Chem. Soc.* **1972**, *94*, 3737.

(4) Eliel, E. L.; Martin, R. J. L. *J. Am. Chem. Soc.* **1968**, *90*, 689.

(5) Jensen, F. R.; Bushweller, C. H.; Beck, B. H. *J. Am. Chem. Soc.* **1969**, *91*, 344.

(6) Schneider, H. J.; Hoppen, V. *Tetrahedron Lett.* **1974**, *7*, 579.

(7) Subbotin, O. A.; Sergeyev, N. M. *J. Am. Chem. Soc.* **1975**, *97*, 1080.

(8) Chu, P.-S.; True, N. S. *J. Phys. Chem.* **1985**, *89*, 5613.

(9) Nordon, A.; Harris, R. K.; Yeo, L.; Harris, K. D. M. *Chem. Commun.* **1997**, *10*, 962.

(10) Bovey, F. A.; Anderson, E. W.; Hood, F. P.; Kornegay, R. L. *J. Chem. Phys.* **1964**, *40*, 3099.

(11) Bugay, D. E.; Bushweller, C. H.; Danehey, C. T.; Hoogasian, S.; Blersch, J. A.; Leenstra, W. R. *J. Phys. Chem.* **1989**, *93*, 3908.

(12) Klaboe, P.; Lothe, J. J.; Lunde, K. *Acta Chem. Scand.* **1956**, *10*, 1465.

(13) Rey-Lafon, M.; Rouffi, C.; Camiade, M.; Forel, M. T. *J. Chim. Phys.* **1970**, *67*, 2030.

(14) Rey-Lafon, M.; Forel, M. T. *J. Mol. Struct.* **1975**, *29*, 193.

(15) Christian, S. D.; Grundnes, J.; Klaeboe, P.; Torneng, E.; Woldbaek, T. *Acta Chem. Scand.* **1980**, *34A*, 391.

(16) Fishman, A. I.; Remizov, A. B.; Stolov, A. A. *Zh. Prikl. Spektr.* **1984**, *40*, 604.

(17) Fishman, A. I.; Stolov, A. A.; Remizov, A. B. *Spectrochim. Acta, Part A* **1985**, *41A*, 505.

(18) Fishman, A. I.; Stolov, A. A.; Remizov, A. B. *Spectrochim. Acta, Part A* **1993**, *49A*, 1435.

(19) Van der Veken, B. J.; Herrebout, W. A. *J. Phys. Chem.* **2001**, *105*, 7198.

(20) Bulanin, M. O. *J. Mol. Struct.* **1973**, *19*, 59.

(21) Van der Veken, B. J. In *Low-temperature molecular spectroscopy*; Fausto, R., Ed.; Kluwer Academic Publishers: Dordrecht, 1996; p 371.

(22) *Peakfit*, version 4.01 for WIN32; Jandel Scientific Software (AISN Software, Inc.).

(23) *Origin*, version 6.0; Microcal Software, Inc.

(24) Jorgensen, W. L. *BOSS*, version 4.1; Yale University: New Haven, CT, 1999.

(25) Klimovitskii, A. E.; Remizov, A. B.; Skvortsov, A. I.; Fedorenko, V. Y.; Fishman, A. I. *Zh. Obshch. Khim.* **1998**, *68*, 1860.

(26) Stokr, J.; Shneider, B.; Jakes, J. *J. Mol. Struct.* **1973**, *15*, 87.

(27) McQuarrie, D. A.; Simon, J. D. *Physical Chemistry. A Molecular Approach*; University Science Books: Sausolito, CA, 1997.

(28) Fishman, A. I.; Remizov, A. B.; Stolov, A. A. *J. Mol. Struct.* **1999**, *480−481*, 303.

(29) Ouellette, R. J.; Williams, S. H. *J. Am. Chem. Soc.* **1971**, *93*, 466.

(30) Knox, J. H. *Molecular Thermodynamics. An Introduction to Statistical Mechanics for Chemists*; Wiley-Interscience: London, 1971.

(31) Pratt, L. R.; Hue, C. S.; Chandler, D. *J. Chem. Phys.* **1978**, *68*, 4202.

(32) Pierce, L.; Beecher, J. F. *J. Am. Chem. Soc.* **1966**, *88*, 5406.

(33) Oroczo, M.; Luque, F. *J. Chem. Rev.* **2000**, *100*, 4187.

(34) Levy, R. M.; Gallicchio, E. *Annu. Rev. Phys. Chem.* **1998**, *49*, 531.